

# ASSESSING THE CONTRIBUTION OF AIRBORNE-RETRIEVED CHLOROPHYLL FLUORESCENCE FOR NITROGEN ASSESSMENT IN ALMOND ORCHARDS

Y. Wang <sup>a,\*</sup>, L. Suarez <sup>a,b</sup>, X. Qian <sup>c</sup>, T. Poblete <sup>b</sup>, V. Gonzalez-Dugo <sup>d</sup>, D. Ryu <sup>a</sup>, P.J. Zarco-Tejada <sup>a,b,d</sup>  
\* E-mail address: wang.y@unimelb.edu.au

<sup>a</sup> Department of Infrastructure Engineering, Faculty of Engineering and Information Technology (FEIT), University of Melbourne, Melbourne, VIC 3010, Australia

<sup>b</sup> School of Agriculture and Food, Faculty of Veterinary and Agricultural Sciences (FVAS), University of Melbourne, Melbourne, VIC 3010, Australia

<sup>c</sup> Key Laboratory of Digital Earth Science, Aerospace Information Research Institute, Chinese Academy of Sciences, Beijing, 100094, China

<sup>d</sup> Instituto de Agricultura Sostenible (IAS), Consejo Superior de Investigaciones Cientificas (CSIC), Avenida Menendez Pidal s/n, 14004 Cordoba, Spain

## ABSTRACT

Standard remote sensing methods for nitrogen (N) assessment in precision agriculture rely on empirical relationships built with chlorophyll  $a+b$  ( $C_{ab}$ ) sensitive vegetation indices. Nevertheless, methods of N estimation based on the  $C_{ab}$  vs. N relationships are strongly affected by the saturation of these indices at high N levels, and by canopy structure, shadows and soil background variability. These effects are even more pronounced in heterogeneous orchards where the tree crown structural variability is a major factor that limits the transferability of the algorithms within- and across-tree crop species. Solar-induced fluorescence (SIF) has been proposed in precision agriculture as a plant functional trait related to N due to its link with photosynthesis. However, retrieving SIF from orchards is challenging due to the mixture of sunlit and shaded crown components. The present study explored the retrieval of airborne SIF in almond orchards from hyperspectral imagery, assessing its contribution to the estimation of N. Results show that the assessment of N improved when SIF was coupled to the model estimated  $C_{ab}$  (e.g.,  $C_{ab}+SIF$ ;  $r^2=0.95$ ) as compared with using  $C_{ab}$  alone ( $r^2=0.87$ ).

**Index Terms** - Chlorophyll Fluorescence, SIF, Nitrogen, Hyperspectral, Almond, FluSAIL RTM

## 1. INTRODUCTION

Nitrogen (N) is an important indicator of plant growth and productivity as it is the major limiting factor in photosynthetic capacity [1]. Monitoring N status timely can inform fertilizer management strategy in terms of balancing plant production against economic losses and environmental

effects [2] for sustainable agriculture purposes. Monitoring the spatial and temporal variability of N status at large scales requires rapid and cost-effective remote sensing methods to overcome the limitations of traditional biochemical analyses of leaf tissues.

Traditional remote sensing methods for N assessment are commonly based on empirical models that use structural and chlorophyll-sensitive vegetation indices employing specific spectral bands [3]. Recent studies have proposed the use of plant traits estimated by radiative transfer models (RTMs) for assessing N in homogenous crops [4, 5]. However, the application of these methods to tree orchards is challenging due to the structural complexity of the canopies caused by clumping effects, crown heterogeneity, within-crown shadows, and soil background influence.

Solar-induced chlorophyll fluorescence (SIF) has been shown as a proxy for photosynthetic activities [6, 7] and therefore sensitive to the leaf nutrient levels [8]. A recent study [4] presented SIF as an indicator for N quantification in wheat phenotyping that improved the predictions when coupled to chlorophyll content ( $C_{ab}$ ). However, the physiological dynamics of SIF vs. N may differ considerably between orchard trees and herbaceous crops due to the within-tree structural variability and background effects. In this study, we explored the retrieval of airborne-quantified SIF in almond orchards from hyperspectral imagery, assessing the contribution of SIF and spectral plant traits for N estimation.

## 2. MATERIAL AND METHODS

### 2.1. Study area

The study was conducted in a commercial almond orchard located in northwestern Victoria, Australia. The almond

orchard (Figure 1a) covers approximately 1200 hectares and was planted in 2006 (Northern blocks oriented N-S) and 2007 (Southern blocks with mixed N-S and E-W orientations). Three different varieties comprising Nonpareil (planted in every two rows), Price (planted in every six rows), and Carmel were planted in groups of 6 rows for cross-pollination purposes [9]. All blocks received the same amount of water and nutrient rates across the entire orchard.

## 2.2. Data collection

### 2.2.1. Field measurements and laboratory analyses

A total of 14 homogenous monitoring plots spread across the entire orchard were selected for leaf measurements and sampling purposes, comprising both Nonpareil and Carmel varieties. Leaf measurements were carried out before harvest on 20 fully exposed leaves per tree from each of the monitoring plots, comprising leaf  $C_{ab}$ , anthocyanins ( $A_{nth}$ ), flavonol content and the nitrogen balance index (NBI) using a Dualex 4 Scientific instrument (FORCE-A, Orsay, France), leaf steady-state chlorophyll fluorescence ( $F_t$ ) and leaf reflectance spectra within the visible and NIR region with FluorPen FP 110 and PolyPen RP 400 instruments (PSI, Brno, Czech Republic), respectively. Meanwhile, a total of 50 leaves per variety were collected from each plot for N determination in the laboratory using a LECO Nitrogen Analyzer (LECO Corporation, MI, USA).

### 2.2.2. Airborne hyperspectral imagery

Within a week of field data collection, an airborne campaign was carried out under clear sky conditions on 17<sup>th</sup> February 2020. A hyperspectral VNIR camera (micro-hyperspec model, Headwall Photonics, Fitchburg, MA, USA) and a thermal infrared camera (A655sc model, FLIR systems, Wilsonville, OR, USA) were installed in tandem on an aircraft (Cessna 172R) operated by the HyperSens Laboratory, the University of Melbourne's Airborne Remote Sensing Facility. The imagery was collected at midday flying in the solar plane at 550 m above ground level, yielding 45 cm and 60 cm pixel resolutions for the hyperspectral and thermal imagery, respectively. Raw images were then calibrated and pre-processed as described in Zarco-Tejada, et al. [10]. Reflectance spectra extracted from pure tree crowns (Figure 2a) and radiance extracted from sunlit vegetation pixels at the  $O_2$ -A absorption feature (Figure 2b) were used to quantify the spectral plant traits and SIF employed for the analysis, respectively.

## 2.3. Plant traits retrievals from hyperspectral imagery

Mean reflectance per plot was calculated from pure sunlit pixels (Figure 1b) for the 358 spectral bands acquired by the airborne hyperspectral camera. Reflectance spectra were used to calculate structural and chlorophyll indices, such as NDVI, EVI, MCARI2, CI and TCARI/OSAVI among

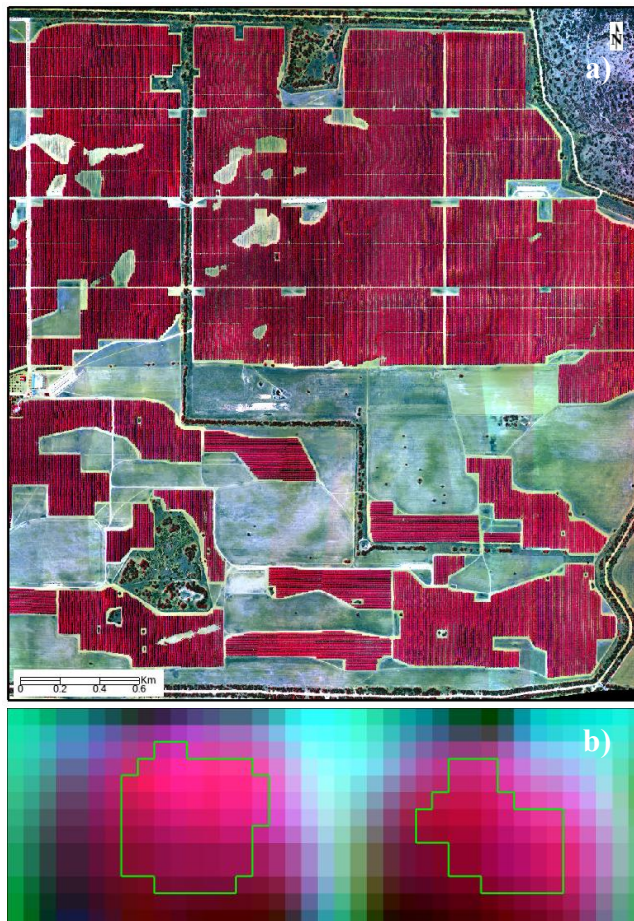


Figure 1. a) False color composite of the hyperspectral imagery acquired over a 1200 ha almond orchard in Victoria, Australia, b) image segmentation applied to individual tree crowns to extract tree crown reflectance and spectral radiance at the  $O_2$ -A spectral feature.

others (see Zarco-Tejada, et al. [10] for a complete list of indices). The spectral reflectance was also used as input for Fluspect-CX leaf [11] coupled with 4SAIL canopy RTM [12] as FluSAIL model to estimate  $C_{ab}$ , carotenoids ( $C_{ar}$ ),  $A_{nth}$ , the de-epoxidation state of the xanthophyll-cycle pigments ( $C_x$ ), dry matter ( $C_{dm}$ ), mesophyll structure (N-struc), leaf area index (LAI), and the leaf inclination distribution ( $LIDF_{a/b}$ ). A look-up table (LUT) containing 50,000 random simulations of FluSAIL was used to retrieve all plant traits for each tree crown at the same time using an artificial neural network model [13].

SIF was quantified from pure sunlit vegetation pixels through the Fraunhofer Line Depth (FLD) principle [14] using three bands (3FLD) [15] from the  $O_2$ -A oxygen absorption feature in the radiance spectra (Figure 2b). The method used the radiance at 762 nm ( $L_{762}$ ) as  $L_{in}$ ,  $L_{750}$  and  $L_{778}$  as  $L_{out}$  and the same spectral bands from the irradiance (E) spectra concurrently measured in the field at the time of flight.

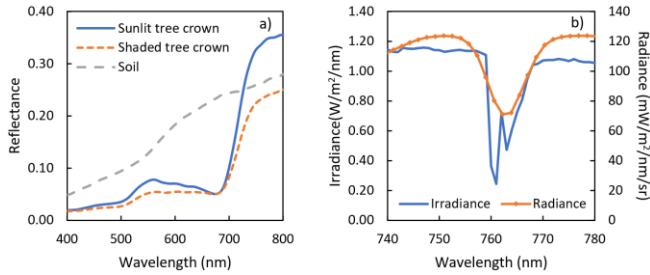


Figure 2. a) Spectra of different scene components extracted from the airborne hyperspectral image: reflectance of soil, sunlit and shaded tree crown pixels, b) radiance spectra extracted from sunlit tree crown pixels at the O<sub>2</sub>-A feature, and field measured irradiance at the time of flight.

#### 2.4. Statistical analysis for nitrogen estimation

Regression random forest machine learning algorithm [16], a computational method that can assess the relative variable importance, was employed to predict N by using the coefficient of determination ( $r^2$ ) and RMSE as the first and second performance measure, respectively. The training and testing steps were performed using the leave-one-out-cross-validation (LOOCV) method for N prediction from a pool of representative parameters, including i) biochemical and structural plant traits retrieved from pure reflectance spectra by FluSAIL model inversion, ii) airborne quantified SIF from the radiance spectra, and iii) crop water stress index (CWSI) calculated from the thermal infrared imagery. For each set of inputs, the variance inflation factor (VIF) and out-of-bag (OOB) predictor importance with sensitivity analysis were employed to suppress the input collinearity and to evaluate the relative contribution of each input to the models, respectively. The final selection of variables for the N prediction model was obtained by filtering the most collinear and less contributing parameters.

### 3. RESULTS

The analysis of the field data illustrated the existing variability of leaf nitrogen and pigment content throughout the orchard (Figure 3), observing the ranges of variation for N, NBI,  $C_{ab}$  and  $A_{nth}$  based on leaf fluorescence quartiles.

Relationships between leaf N concentration vs. airborne NDVI ( $r^2=0.27$ , n.s., Figure 4a) showed that the crown structure was not a major driver in the N variability throughout the orchard. While TCARI/OSAVI chlorophyll index was better related to N ( $r^2=0.53$ ,  $p<0.05$ , Figure 4b) than any other spectral index. Nevertheless, plant traits estimated by RTM inversion such as  $C_{ab}$  ( $r^2=0.70$ ,  $p<0.001$ , Figure 4c) and airborne SIF ( $r^2=0.64$ ,  $p<0.001$ , Figure 4d) yielded stronger relationships than standard indices against leaf N concentration. Airborne-quantified  $C_{ab}$  and SIF also showed statistically significant relationships with the equivalent field-measured leaf  $C_{ab}$  ( $r^2=0.64$ ,  $p<0.001$ ) and leaf Ft ( $r^2=0.61$ ,  $p<0.001$ ) (data not shown).

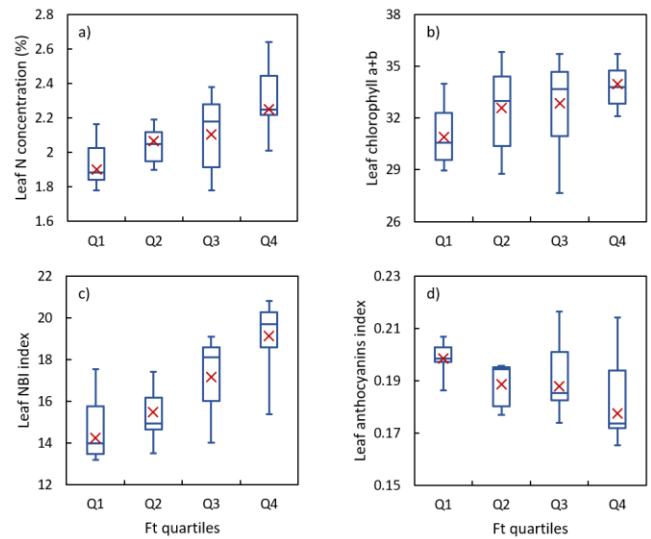


Figure 3. Ranges of variation for a) leaf nitrogen concentration, b) chlorophyll  $a+b$ , c) nitrogen balance index and d) anthocyanins content based on leaf fluorescence quartiles. Crossing line through the box and marker 'x' refer to the median and mean value, respectively. Box amplitude refers to the second and third quartiles' limits.

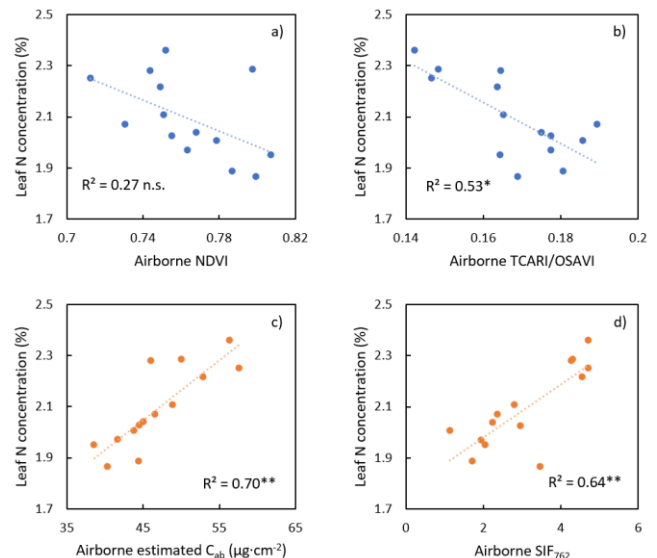


Figure 4. Relationships between nitrogen concentration and a) airborne NDVI, b) airborne TCARI/OSAVI, c) chlorophyll  $a+b$  estimated by RTM inversion, and d) SIF quantified at O<sub>2</sub>-A using the 3FLD *in-filling* method from the airborne radiance spectra.  
\* $p$ -value $<0.05$ ; \*\* $p$ -value $<0.001$ ; n.s.= not significant.

The relative contribution of each plant trait for estimating leaf nitrogen assessed by the OOB predictor importance analysis showed that the model estimated  $C_{ab}$  and airborne-quantified SIF were the spectra plant traits contributing the most (Figure 5), followed by  $C_{ar}$ ,  $C_x$  and  $A_{nth}$  biochemical constituents. The structural trait LAI, and

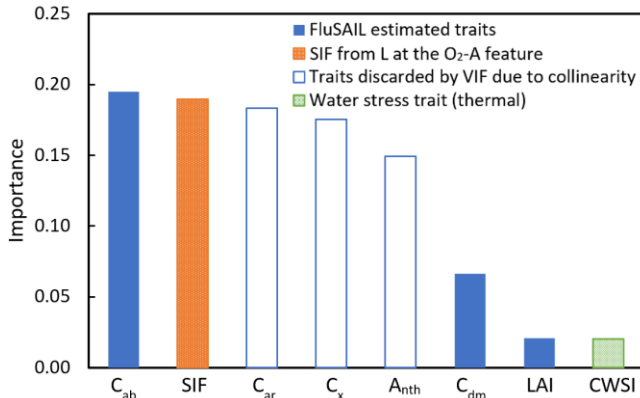


Figure 5. Relative contribution of each input to the model built to estimate N concentration from the pool of FluSAIL model inverted plant traits, airborne quantified SIF, and the water stress indicator CWSI.

the water stress indicator CWSI showed a weak contribution to N variability. However, the statistical analysis showed that C<sub>ab</sub> and SIF were not strongly collinear, while C<sub>ar</sub>, C<sub>x</sub> and A<sub>nth</sub> were discarded after presenting a VIF>10 with C<sub>ab</sub>. Results also showed that the model performance for assessing N content was improved when coupling airborne SIF with any plant traits, particularly with C<sub>ab</sub> derived from RTM inversion, increasing r<sup>2</sup> from 0.87 to 0.95 and reducing the RMSE from 0.064 to 0.044. As a result, the model consisting of C<sub>ab</sub> and airborne SIF together explained 95% of the N variability in the almond orchard comprising different varieties, ages, and water status levels.

#### 4. CONCLUSIONS

This study shows that airborne-retrieved chlorophyll fluorescence improves the prediction of leaf nitrogen content in almond orchards when coupled with plant traits. Notably, when airborne SIF is coupled to C<sub>ab</sub> estimated by radiative transfer simulations, the model explained 95% of the variability of nitrogen in the almond orchard. The analysis showed that C<sub>ab</sub> and SIF were non-collinear, while other biochemical constituents such as C<sub>ar</sub>, C<sub>x</sub> and A<sub>nth</sub> estimated from RTM inversion were discarded by the VIF analysis as they presented strong collinearity with C<sub>ab</sub>. This study demonstrates the interest of using SIF coupled to C<sub>ab</sub> for the assessment of N in structurally complex canopies such as almond orchards for precision agriculture purposes.

#### 5. ACKNOWLEDGMENTS

The authors gratefully acknowledge McPherson Family and Invergowrie Foundation for the financial support and the assistant from the Mallee Regional Innovation Centre (MRIC). Special thanks to Brian Slater for allowing this research to be carried out in the Aroona Farms and Rafael Romero, David Notario and Alberto Hornero from QuantaLab IAS-CSIC (Spain) for laboratory support.

#### 6. REFERENCES

- [1] J. R. Evans, "Photosynthesis and nitrogen relationships in leaves of C 3 plants," *Oecologia*, vol. 78, no. 1, pp. 9-19, 1989.
- [2] F. J. Stevenson and M. A. Cole, *Cycles of soils: carbon, nitrogen, phosphorus, sulfur, micronutrients*. John Wiley & Sons, 1999.
- [3] P. Hansen and J. Schjoerring, "Reflectance measurement of canopy biomass and nitrogen status in wheat crops using normalized difference vegetation indices and partial least squares regression," *Remote sensing of environment*, vol. 86, no. 4, pp. 542-553, 2003.
- [4] C. Camino, V. González-Dugo, P. Hernández, J. Sillero, and P. J. Zarco-Tejada, "Improved nitrogen retrievals with airborne-derived fluorescence and plant traits quantified from VNIR-SWIR hyperspectral imagery in the context of precision agriculture," *International journal of applied earth observation and geoinformation*, vol. 70, pp. 105-117, 2018.
- [5] F. Baret, V. Houlès, and M. Guerif, "Quantification of plant stress using remote sensing observations and crop models: the case of nitrogen management," *Journal of Experimental Botany*, vol. 58, no. 4, pp. 869-880, 2007.
- [6] P. J. Zarco-Tejada, A. Catalina, M. González, and P. Martín, "Relationships between net photosynthesis and steady-state chlorophyll fluorescence retrieved from airborne hyperspectral imagery," *Remote Sensing of Environment*, vol. 136, pp. 247-258, 2013.
- [7] G. Krause and E. Weis, "Chlorophyll fluorescence and photosynthesis: the basics," *Annual review of plant biology*, vol. 42, no. 1, pp. 313-349, 1991.
- [8] N. Tremblay, Z. Wang, and Z. G. Cerovic, "Sensing crop nitrogen status with fluorescence indicators. A review," *Agronomy for sustainable development*, vol. 32, no. 2, pp. 451-464, 2012.
- [9] W. Asai, W. Micke, D. Kester, and D. Rough, "The evaluation and selection of current varieties," *Almond production manual*, pp. 52-60, 1996.
- [10] P. Zarco-Tejada *et al.*, "Previsual symptoms of Xylella fastidiosa infection revealed in spectral plant-trait alterations," *Nature Plants*, vol. 4, no. 7, pp. 432-439, 2018.
- [11] N. Vilfan *et al.*, "Extending FluSpec to simulate xanthophyll driven leaf reflectance dynamics," *Remote sensing of environment*, vol. 211, pp. 345-356, 2018.
- [12] W. Verhoef, L. Jia, Q. Xiao, and Z. Su, "Unified optical-thermal four-stream radiative transfer theory for homogeneous vegetation canopies," *IEEE Transactions on geoscience and remote sensing*, vol. 45, no. 6, pp. 1808-1822, 2007.
- [13] M. H. Hassoun, *Fundamentals of artificial neural networks*. MIT press, 1995.
- [14] J. A. Plascyk and F. C. Gabriel, "The Fraunhofer line discriminator MKII-an airborne instrument for precise and standardized ecological luminescence measurement," *IEEE Transactions on Instrumentation and measurement*, vol. 24, no. 4, pp. 306-313, 1975.
- [15] S. W. Maier, K. P. Günther, and M. Stellmes, "Sun-induced fluorescence: A new tool for precision farming," *Digital imaging and spectral techniques: Applications to precision agriculture and crop physiology*, vol. 66, pp. 207-222, 2004.
- [16] L. Breiman, "Random forests," *Machine learning*, vol. 45, no. 1, pp. 5-32, 2001.